

Figure 13. Comparison between defoliation data for the Horopito site derived from an aerial photograph. A-the area covered by the data is shown in the colour-infrared image. B-canopy defoliation data derived from the red/near-infrared VI, according to the relationship between defoliation and the VI developed for kamahi. In comparison with what can be visually identified in the colour-infrared image, defoliation is clearly over-estimated by the red/near-infrared index, primarily because rimu are rated as dead trees by this index. C-canopy defoliation data derived from a green/red band ratio (again using the relationship between defoliation and this ratio developed for kamahi). This provides a significantly more realistic portrayal of forest condition at the site. The defoliation key is the same as in Fig. 12.

7. Bibliography

- Carter, G.A.; Dell, T.R.; Cibula, W.G. 1996. Spectral characteristics and digital imagery of a pine needle blight in the southeastern United States. *Canadian Journal of Forest Research* 26: 402-407.
- Crippen, R.E. 1988. The dangers of underestimating the importance of data adjustments in band ratioing. *International Journal of Remote Sensing* 9(4): 767-776.
- Curran, P.J. 1980. Multispectral remote sensing of vegetation amount. *Progress in Physical Geography* 4: 315.
- Dymond, J.R.; Trotter, C.M. 1997. Measuring directional effects of vegetation reflectance with a digital camera. *Applied Optics* 36(18): 4314-4319.
- Ekstrand, S. 1996. Landsat TM-based forest damage assessment: correction for topographic effects. *Photogrammetric Engineering and Remote Sensing* 62(2): 151-161.
- Kimes, D.S.; Newcomb, W.W.; Nelson, R.F.; Schutt, J.B. 1986. Directional reflectance distributions of a hardwood and pine forest canopy. *IEEE Transactions on Geoscience and Remote Sensing* GE-24(2): 281-293.
- Lambert, N.J.; Ardö, J. Rock, B.N.; Vogelmann, J.E. 1995. Spectral characterisation and regression-based classification of forest damage in Norway spruce stands in Czech Republic using Landsat Thematic Mapper data. *International Journal of Remote Sensing* 16(7): 1261-1287.
- Leprieur, C.E.; Durand, J.M. 1988. Influence of topography on forest reflectance using Landsat Thematic Mapper and digital terrain data. *Photogrammetric Engineering and Remote Sensing* 54(4): 491-496.
- McCull, R. 1995. Personal communication. Conservation Sciences Centre, Department of Conservation, Wellington.
- Payton, I.J.; Pekelharing, C.J.; Frampton, C.M. 1997. Foliar browse index: a method for monitoring possum damage to forests and rare or endangered plant species. *Landcare Research Contract Report LC9697/60*: 62 p, Landcare Research, Lincoln.
- Ranson, K.J.; Daugherty, C.S.T.; Biehl, L.L. 1986. Sun angle, view angle, and background response effects of spectral response of simulated Balsam Fir canopies. *Photogrammetric Engineering and Remote Sensing* 52(5): 649-658.
- Smith, J.A.; Lin, T.L.; Ranson, K.J. 1980. The Lambertian assumption and Landsat data. *Photogrammetric Engineering and Remote Sensing* 46(9): 1183-1189.
- Syrén, P. 1994. Reflectance anisotropy for nadir observations of coniferous forest canopies. *Remote Sensing of Environment* 49: 72-80.
- Trotter, C.M. 1992a. Estimating possum browse damage to lowland indigenous forest using remote sensing—a feasibility study. *Proceedings of the 6th Australasian Remote Sensing Conference* 1: 400-405. Wellington, New Zealand.
- Trotter, C.M. 1992b. Mapping possum damage using remote sensing—a feasibility study. *DSIR Land Resources Technical Report 92/34*. Lower Hutt, New Zealand.
- Tucker, C.J. 1979. Red and photographic infrared linear combinations for monitoring vegetation. *Remote Sensing of Environment* 8: 127-150.
- Woodham, R.J.; Gray, M.H. 1987. An analytic method for radiometric correction of satellite multispectral scanner data. *IEEE Transactions on Geoscience and Remote Sensing* 25(3): 258-271.

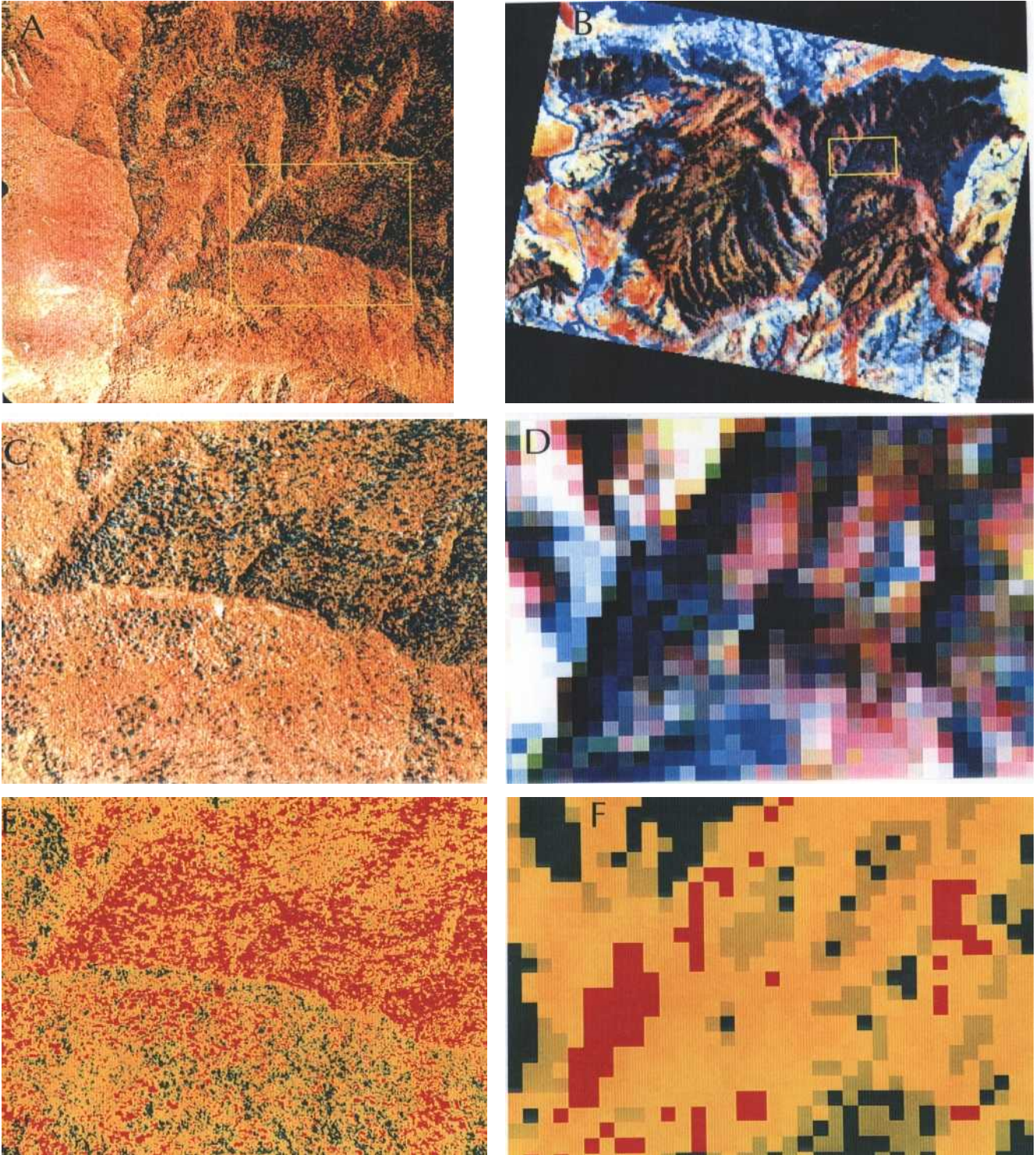


Figure 14. Comparison of data for the Hihitahi site, derived from an aerial photograph and a satellite image. A, B-the location of the study site is outlined in yellow on an extract of a colour-infrared photo and a Landsat TM image, respectively. C, D-the area covered approximately by the site only, illustrating the spatially coarse nature of the satellite data (30 m pixels) in comparison with the scale of variation within the forest. E, F-canopy defoliation data derived from a red/near-Infrared VI using photographic and satellite data, respectively. The relationship used between defoliation and the VI is that developed for kamahi. The defoliation key is the same as in Fig. 12.

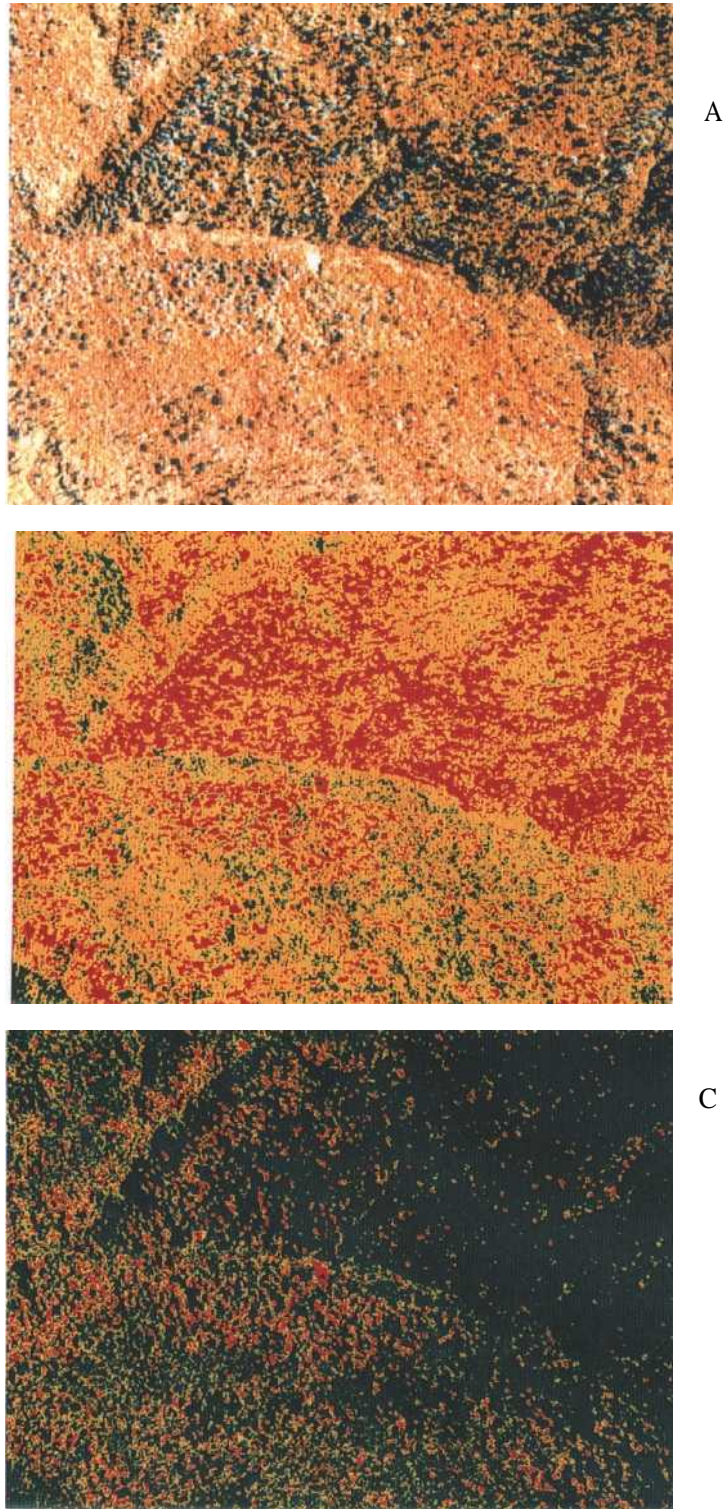


Figure 15. Comparison between defoliation data derived from an aerial photograph, for the Hihitahi site. A-the area from which the data are derived is shown as a colour-infrared image. B-canopy defoliation data derived from the red/near-infrared VI, according to the relationship between defoliation and the VI developed for kamahi. In comparison with what can be visually identified in the colour-infrared image, defoliation is clearly greatly over-estimated by the red/near-infrared index, primarily because undamaged conifers and horopito shrubland are rated as dead trees by this index. C-defoliation data derived from a green/red band ratio (again using the relationship between defoliation and this ratio developed for kamahi). This provides a significantly more realistic portrayal of forest condition at the site. The defoliation key is the same as in Fig. 12.